Journal of Biomechanics 47 (2014) 2556–2562

Contents lists available at ScienceDirect

Journal of Biomechanics

journal homepage: www.elsevier.com/locate/jbiomech
www.JBiomech.com

Three-dimensional knee joint contact forces during walking in unilateral transtibial amputees

Anne K. Silverman [a,*], Richard R. Neptune [b]

[a] Department of Mechanical Engineering, Colorado School of Mines, 1500 Illinois Street, Golden, CO 80401, USA
[b] Department of Mechanical Engineering, The University of Texas at Austin, Austin, TX 78712, USA

ARTICLE INFO

Article history:
Accepted 4 June 2014

Keywords:
Biomechanics
Locomotion
Below-knee
Forward dynamics
Joint loading

ABSTRACT

Individuals with unilateral transtibial amputations have greater prevalence of osteoarthritis in the intact knee joint relative to the residual leg and non-amputees, but the cause of this greater prevalence is unclear. The purpose of this study was to compare knee joint contact forces and the muscles contributing to these forces between amputees and non-amputees during walking using forward dynamics simulations. We predicted that the intact knee contact forces would be higher than those of the residual leg and non-amputees. In the axial and mediolateral directions, the intact and non-amputee legs had greater peak tibio-femoral contact forces and impulses relative to the residual leg. The peak axial contact force was greater in the intact leg relative to the non-amputee leg, but the stance phase impulse was greater in the non-amputee leg. The vasti and hamstrings muscles in early stance and gastrocnemius in late stance were the largest contributors to the joint contact forces in the non-amputee and intact legs. Through dynamic coupling, the soleus and gluteus medius also had large contributions, even though they do not span the knee joint. In the residual leg, the prosthesis had large contributions to the joint forces, similar to the soleus in the intact and non-amputee legs. These results identify the muscles that contribute to knee joint contact forces during transtibial amputee walking and suggest that the peak knee contact forces may be more important than the knee contact impulses in explaining the high prevalence of intact leg osteoarthritis.

1. Introduction

Individuals with unilateral transtibial amputations have altered gait mechanics and muscle coordination patterns relative to non-amputees (e.g., Fey et al., 2010; Silverman and Neptune, 2012), which may lead to the onset of joint disorders with prolonged use. For example, transtibial amputees have an increased prevalence and early onset of osteoarthritis (OA) and pain in the intact leg knee joint relative to the residual leg and non-amputees (Burke et al., 1978; Lemaire and Fisher, 1994; Melzer et al., 2001; Norvell et al., 2005; Struyf et al., 2009). However, the biomechanical mechanisms that contribute to the increased prevalence remain unclear.

The etiology of OA is not completely understood, but is partially attributed to increased and/or atypical joint loading (Maly, 2009; Morgenroth et al., 2012). Thus, the increased prevalence of OA in the intact knee of amputees may be a result of greater joint loading relative to the residual leg and non-amputees. Studies of amputee walking have shown elevated intact leg ground reaction forces (GRFs) and joint kinetics relative to the residual leg (Nolan et al., 2003; Royer and Koenig, 2005; Sanderson and Martin, 1997; Silverman et al., 2008) and non-amputee subjects (Nolan and Lees, 2000). Amputees also often have greater stance times on the intact leg relative to the residual leg (e.g., Isakov et al., 2000; Nolan et al., 2003), which may result in greater force impulses in the intact leg knee joint. Identifying differences in knee joint loading in amputees relative to non-amputees is important for understanding the potential biomechanical mechanisms that contribute to the high prevalence of OA in this population.

Recent work has investigated knee joint intersegmental forces across a range of walking speeds and found no significant differences between the intact and residual legs or between the intact and non-amputee legs (Fey and Neptune, 2012). However, inverse dynamics-based intersegmental forces often underestimate joint contact forces, as they do not account for the compressive forces from muscles (Zajac et al., 2002). In addition, altered muscle coordination patterns (Fey et al., 2010; Powers et al., 1998; Winter and Sienko, 1988) and increased co-contraction of the residual leg vasti and hamstring muscles (e.g., Culham et al., 1986; Isakov et al., 2001; Pinzur et al., 1991) in transtibial amputee walking likely influence the knee joint contact forces.

* Corresponding author. Tel.: +1 303 384 2162; fax: +1 303 273 3602.
E-mail address: asilverm@mines.edu (A.K. Silverman).

http://dx.doi.org/10.1016/j.jbiomech.2014.06.006
0021-9290/

A significant challenge to investigating joint contact forces is the extreme difficulty, if not impossibility, of measuring them *in vivo*. In contrast, musculoskeletal modeling and simulation provide an ideal framework to estimate joint contact forces and quantify the contributions of individual muscles during dynamic movements (e.g., Sasaki and Neptune, 2010; Shelburne et al., 2006; Zajac et al., 2003). The gastrocnemius and soleus muscles have been shown to be large contributors to the knee joint contact force in non-amputee walking (Lin et al., 2010; Sasaki and Neptune, 2010; Shelburne et al., 2006), which may lead to asymmetric knee loading in unilateral transtibial amputees because they no longer have the functional use of these muscles in the residual leg.

The objective of this study was to investigate differences in knee joint contact forces in both the residual and intact legs relative to non-amputees during steady-state walking using three-dimensional musculoskeletal models and forward dynamics simulations. We expected that the peak knee contact forces and stance phase force impulses would be greater in the intact knee relative to the residual leg and non-amputees. In addition, individual muscle contributions to the knee contact forces were quantified to identify the potential biomechanical mechanisms that may contribute to the increased prevalence of OA in the intact knee.

2. Methods

2.1. Experimental data collection

Previously-collected kinematic, GRF and electromyographic (EMG) data were used to generate the forward dynamics simulations (Fey et al., 2010; Silverman et al., 2008). Briefly, the data were collected from 14 individuals with transtibial amputation and 10 non-amputees walking overground at 1.2 ± 0.06 m/s (Table 1). Subjects provided informed consent to participate in the experimental protocol approved by an Institutional Review Board. Kinematic data were collected at 120 Hz and GRF and EMG data were collected at 1200 Hz. EMG data were collected using surface electrodes from eight intact-leg muscles and five residual-leg muscles (Table 2). Kinematic data were low-pass filtered using a 4th-order Butterworth filter with a cutoff frequency of 6 Hz. GRF data were similarly filtered with a cutoff frequency of 20 Hz. EMG data were demeaned, rectified, high-pass filtered with a cutoff frequency of 40 Hz, and then low-pass filtered with a cutoff frequency of 4 Hz. Data were normalized to the gait cycle and averaged across subjects for both the amputee and non-amputee groups.

2.2. Musculoskeletal model

A three-dimensional musculoskeletal model was developed using SIMM (Musculographics, Inc.) and has been previously described in detail (Silverman and Neptune, 2012). The model had 14 rigid body segments and 23 degrees-of-freedom. Body segments included a right and left thigh, shank, patella, talus, calcaneus and toes, as well as a head-arms-trunk (HAT) segment and pelvis. Degrees-of-freedom included a six degree-of-freedom joint between the ground and pelvis, three rotational degrees-of-freedom between the pelvis and HAT, and three rotational degrees-of-freedom between the pelvis and each thigh. Single rotational degrees-of-freedom were defined at the knee, ankle, subtalar and metatarsalphalangeal joints. Passive torques were applied at each joint to represent ligament and passive tissue forces (Anderson, 1999; Davy and Audu, 1987). Foot-ground contact was modeled using 31 independent visco-elastic elements with coulomb friction on the bottom of each foot (Neptune et al., 2000). The dynamic equations-of-motion were generated using SD/FAST (PTC).

The model included 38 Hill-type musculotendon actuators per leg, with geometry based on Delp et al. (1990) and force-length-velocity relationships (Zajac, 1989). The excitation for each muscle was defined using a bimodal excitation pattern (e.g., Silverman and Neptune, 2012). Muscle activation/deactivation dynamics were modeled using a first-order differential equation (Raasch et al., 1997) with time constants based on Winters and Stark (1988). For the non-amputee model, symmetric muscle excitation patterns were used between legs.

To model the unilateral transtibial amputees, the mass and inertial properties of the shank were modified and muscles crossing the ankle joint were removed to represent the residual leg in an amputee (Silverman and Neptune, 2012). The prosthesis was modeled using a second-order torsional spring with damping at the ankle joint (Silverman and Neptune, 2012).

2.3. Optimization framework

A simulated annealing optimization framework (Goffe et al., 1994) was used to generate three forward dynamics simulations of the stance phase when the joint contact forces are the highest (Silverman and Neptune, 2012). The simulations consisted of amputee residual leg stance, amputee intact leg stance and non-amputee left leg stance. To generate simulations emulating the human subject walking mechanics, the optimization cost function (Eq. (1)) consisted of the

Table 2
Muscles included in the musculoskeletal model and corresponding muscle groups. '*' indicates muscles that were not included in the residual leg of the amputee model and '$^{\Delta}$' indicates that electromyographic data were available for the muscle.

Muscle	Muscle group
Iliacus	IL
Psoas	
Adductor longus	AL
Adductor brevis	
Pectineus	
Quadratus femoris	
Adductor magnus (superior, middle, and inferior compartments)	AM
Sartorius	SAR
$^{\Delta}$ Rectus femoris	RF
Vastus medialis	VAS
Vastus intermedius	
$^{\Delta}$ Vastus lateralis	
$^{\Delta}$ Gluteus medius (anterior, middle and posterior compartments)	GMED
Gluteus minimus (anterior, middle and posterior compartments)	
Gemellus	
Piriformis	
Tensor fascia lata	TFL
$^{\Delta}$ Gluteus maximus (superior, middle and inferior compartments)	GMAX
Semimembranosus	HAM
Semitendinosus	
Gracilis	
$^{\Delta}$ Biceps femoris long head	
Biceps femoris short head	BFSH
* $^{\Delta}$ Gastrocnemius (medial and lateral heads)	GAS
* $^{\Delta}$ Soleus	SOL
*Tibialis posterior	
*Flexor digitorum longus	
* $^{\Delta}$ Tibialis anterior	TA
*Extensor digitorum longus	

Table 1
Mean (standard deviation) amputee and non-amputee group characteristics.

	Age (years)	Body mass (kg)	Height (m)	Time since amputation (years)	Etiology	Prosthetic foot type
Amputees	45.1 (9.1)	90.6 (18.6)	1.76 (0.1)	5.6 (2.9)	11 Traumatic 3 Vascular	9 ESAR 5 SACH
Non-amputees	34.1 (13.0)	70.9 (13.6)	1.76 (0.1)	–	–	–

difference between the experimental and simulated joint kinematics and GRFs as well as the muscle stress of all muscles in the model:

$$J = \sum_{j=1}^{p}\sum_{i=1}^{n} w_j \frac{(Y_{ij}-\hat{Y}_{ij})^2}{SD_{ij}^2} + \sum_{m=1}^{q}\sum_{i=1}^{n} w_m \frac{F_{im}}{PCSA_m} \quad (1)$$

where w_j is a weighting factor of variable j, Y_{ij} is the experimental measurement of variable j at time step i, $\hat{Y}_{ij}$ is the corresponding simulation value, and SD_{ij}^2 is the average variability of variable j across trials. w_m is a weighting factor of muscle m, F_{im} is the force of muscle m and $PCSA_m$ is the physiological cross-sectional area of muscle m. Muscle stress was used to help minimize unnecessary co-contraction that would influence the joint contact forces. The muscle excitation patterns were constrained to closely match the measured EMG patterns and the optimization algorithm fine-tuned the excitation timing and magnitude within these constraints to minimize Eq. (1).

2.4. Muscle contributions to the knee joint contact force

The three-dimensional tibio-femoral joint contact forces were determined from the joint intersegmental force and compressive forces from the muscles crossing the joint using SD/FAST. Joint loading was quantified by the peak value and the time integral of the tibio-femoral joint contact force on the tibia (expressed in the tibial reference frame) over the stance phase in each coordinate direction. The anterior/posterior (A/P), axial and mediolateral (M/L) joint contact impulses were compared between the amputee residual leg, amputee intact leg and non-amputee left leg.

In addition, the individual muscle and prosthesis contributions to the joint contact forces were quantified. To determine these contributions, the total joint contact force was calculated for the complete system at time step i. Then, at step $i-1$ an individual muscle force and that muscle's contribution to the GRF were removed from the system. Similarly, for the prosthesis, the passive torque at the ankle and its contribution to the GRF were removed from the system. Integrating forward in time, the new joint contact force was determined at time step i. The difference in the contact force between the full and reduced systems at time step i was the individual muscle or prosthesis contribution to the joint contact force. For interpretation, the muscles in the model were arranged into 14 muscle groups based on anatomical location and function (Table 2). This analysis has been previously performed to find individual muscle contributions to the hip intersegmental force (Zajac et al., 2003) and knee joint contact force (Sasaki and Neptune, 2010) during non-amputee walking.

3. Results

3.1. Walking simulation results

The experimental kinematics and GRFs were reproduced by the walking simulations in that the three stance simulations largely remained within two standard deviations (2SD) of the experimental walking trials. The residual leg stance simulation had an average difference of 7.11° (2SD=10.54°) across all degrees of freedom and 5.65% body weight (BW, 2SD=5.35%BW) from the average amputee experimental data. The intact leg stance simulation had an average difference of 5.27° (2SD=10.41°) and 5.07%BW (2SD=5.32%BW) from the experimental data. The non-amputee left leg stance simulation had an average difference of 4.27° (2SD=10.82°) and 5.15%BW (2SD=6.07%BW) from the average non-amputee experimental data.

3.2. A/P contact forces

The net A/P joint contact force was directed anteriorly throughout stance for all three legs (Fig. 1). Peak anterior forces were the largest for the intact leg, followed by the residual and non-amputee legs, respectively (Table 3). The A/P impulse (area under the force curve) was the largest in the residual leg (Table 4; Fig. 1, shaded area). The residual leg A/P contact force was larger in mid-stance relative to the intact and non-amputee legs. VAS, HAM and RF had large contributions to the anterior force in early stance in all three legs. In late stance, SOL contributed to the anterior force in the intact and non-amputee legs, whereas the prosthesis contributed to a greater extent in the residual leg. GAS contributed posteriorly in the intact and non-amputee legs, which was not present in the residual leg.

Table 3
Peak tibio-femoral joint contact forces in % body weight (% BW) for the residual, intact and non-amputee simulations. Note that forces are acting on the tibia. Positive was defined in the anterior, superior and medial directions. The largest peak forces in each coordinate direction are in bold.

	Residual	Intact	Non-amputee
Anterior/posterior	155.36	**183.28**	113.89
Axial	−310.10	**−405.55**	−373.10
Mediolateral	16.11	20.74	**26.70**

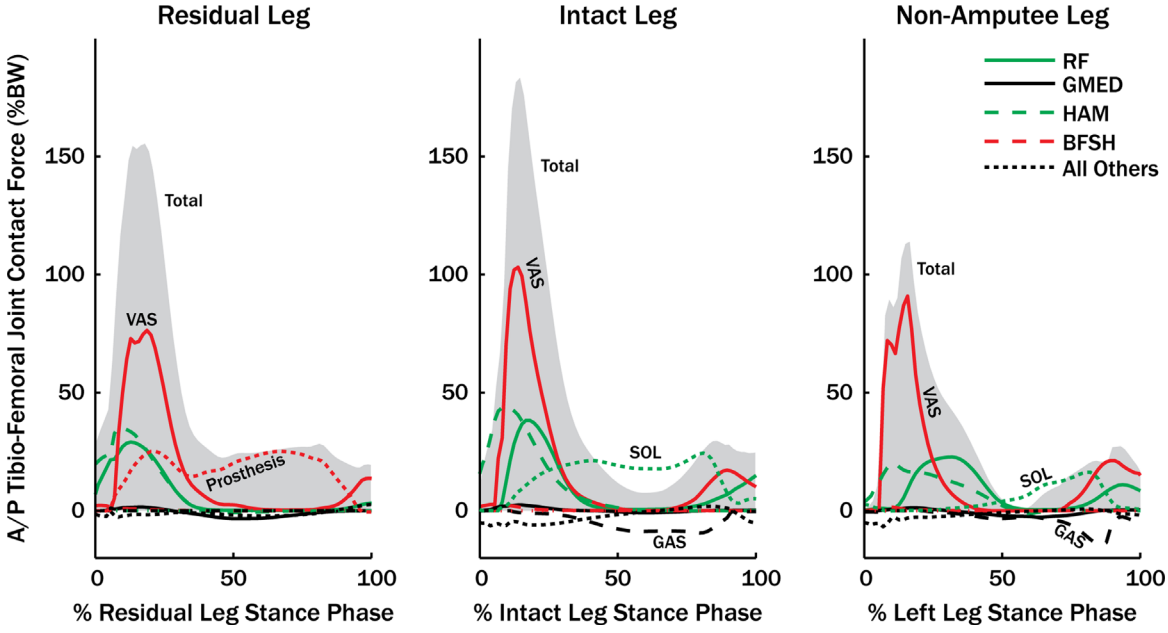

Fig. 1. Ipsilateral leg muscle group contributions to the anterior/posterior (A/P) tibio-femoral joint contact force over the stance phase. Forces are acting on the tibia and anterior is defined as positive.

3.3. Axial contact forces

The total axial tibio-femoral joint contact force was directed downward on the tibia. The peak axial force was the largest in the intact leg and the smallest in the residual leg (Table 3). In contrast, the net impulse was the largest in the non-amputee leg (Table 4; Fig. 2, shaded area) and the intact leg impulse was higher than that of the residual leg. In early stance, all three legs had large contributions from VAS and HAM. In late stance, the non-amputee and intact leg force was dominated by contributions from the ankle plantarflexors (SOL and GAS). In the residual leg, the prosthesis contributed substantially in late stance, but had a smaller net contribution compared to the plantarflexors in the other legs.

3.4. M/L contact forces

The tibio-femoral force was directed medially on the tibia for the majority of stance (Fig. 3). The peak medial force was the largest in the non-amputee leg, followed by the intact and residual legs, respectively. The net impulse was largest in the intact leg and smallest in the residual leg. In all three simulations, VAS contributed medially and was the largest contributor in the first half of stance. Contributions of GMED were directed laterally in all three legs. GAS had a large medial contribution from mid to late stance in the intact and non-amputee legs. The prosthesis contributed medially for the majority of stance, but had a much smaller contribution relative to GAS.

4. Discussion

The intact and non-amputee peak forces and impulses were larger than in the residual leg in the axial and *M/L* directions (Tables 3 and 4). The peak anterior force in the intact leg was also larger than the residual leg. These results agreed with our expectations and are supported by previous experimental studies that have shown the greater GRFs on the intact and non-amputee legs relative to the residual leg (Nolan et al., 2003; Sanderson and Martin, 1997; Silverman et al., 2008). The average axial and M/L force magnitudes were greater in the intact and non-amputee legs relative to the residual leg, which resulted in the greater impulses. In general, muscles crossing the knee joint had the largest contributions to the knee joint contact force in all three directions (Figs. 1–3). For example, the largest contributors in the non-amputee and intact legs were from VAS in early stance and GAS in late stance, which was similar to previous analyses of non-amputee walking (Lin et al., 2010; Sasaki and Neptune, 2010; Shelburne et al., 2006; Winby et al., 2009). However, muscles that did not cross the knee joint, such as SOL and GMED, also substantially contributed to the knee joint forces through dynamic coupling, which is consistent with previous analyses of non-amputee walking (Sasaki and Neptune, 2010).

Loading differences between the residual, intact and non-amputee legs were largely due to altered contributions of the prosthesis relative to the ankle plantar flexors. For example, the residual leg had the largest joint contact impulse in the anterior direction. GAS had substantial posterior contributions in the intact and non-amputee legs, which was not present in the residual leg (Fig. 1). In addition, SOL and the prosthesis both contributed anteriorly, but the prosthesis contribution was larger resulting in a larger anterior impulse in the residual leg. In the axial direction, the prosthesis contributed to a lesser extent in the residual leg compared to the plantarflexors in the intact and non-amputee legs (Fig. 2). Similarly, in the M/L direction the medial contribution of the prosthesis in the residual leg was much smaller than that of GAS in late stance, which dominated the impulse in the intact and non-amputee legs (Fig. 3). Overall, the contributions of the prosthesis were similar in timing and direction to SOL, which was consistent with previous analyses of muscle and prosthesis function in amputee gait (Silverman and Neptune, 2012; Zmitrewicz et al., 2007).

In the axial direction, the intact peak force was the largest, but the non-amputee leg had a greater force impulse relative to the intact leg. The intact leg stance time (0.82 s) was similar to the non-amputee leg stance time (0.80 s). Thus, the greater axial impulse in the non-amputee leg resulted from a greater overall average axial force. The peak results agree with our expectations of greater loading in the intact knee relative to non-amputees, but the impulse results are not what we expected. The greater intact leg peak forces and stance impulses were expected given the association of OA development with increased loading as well as the greater prevalence of OA in amputees relative to non-amputees (Suri et al., 2012). The greater peak value in the intact leg relative to the non-amputee leg was largely a result of the HAM contribution in early stance (Fig. 2), which is consistent with

Table 4
Total tibio-femoral joint contact impulses and contributions from ipsilateral muscle groups in % body weight-seconds (% BW-s) over the stance phase for the residual, intact and non-amputee simulations. Note that impulses are acting on the tibia. Positive was defined in the anterior, superior and medial directions. The largest total impulses in each coordinate direction are in bold.

Muscle group	Anterior/posterior			Axial			Mediolateral		
	Residual	Intact	Non-amputee	Residual	Intact	Non-amputee	Residual	Intact	Non-amputee
IL	0.52	0.26	0.26	0.43	1.12	1.02	0.19	0.00	0.01
AL	0.22	−0.10	−0.07	1.03	1.24	0.98	1.05	1.05	0.73
AM	−0.08	−0.10	−0.09	−0.17	−0.15	−0.02	0.17	0.33	0.28
SAR	−0.17	0.71	0.40	−7.85	−5.96	−0.99	−0.37	−0.42	−0.07
RF	5.34	7.33	6.37	−10.52	−12.71	−18.60	0.03	0.13	0.27
VAS	12.74	15.04	13.24	−26.51	−27.66	−29.65	4.12	4.14	4.60
GMED	−0.74	0.23	−0.52	−4.79	−5.86	−10.82	−3.89	−3.27	−4.49
TFL	−1.14	−0.98	−0.62	−13.41	−9.58	−6.75	1.07	0.60	0.47
GMAX	−0.20	−0.21	−0.22	−2.40	−3.79	−3.61	−0.10	0.13	−0.04
HAM	5.67	7.94	4.71	−16.91	−23.23	−30.45	0.44	−0.10	0.76
BFSH	0.18	0.37	0.15	−1.35	−2.36	−1.91	−0.11	−0.20	−0.15
GAS	–	−3.60	−2.74	–	−56.49	−67.73	–	5.41	5.90
SOL	–	11.86	3.82	–	−26.92	−10.84	–	0.66	−0.31
TA	–	−1.56	−0.88	–	2.08	0.50	–	−0.22	−0.07
Prosthesis	13.18	–	–	−32.66	–	–	1.73	–	–
Total impulse	**39.16**	36.98	24.83	−123.84	−172.84	**−190.28**	4.92	**8.58**	7.61

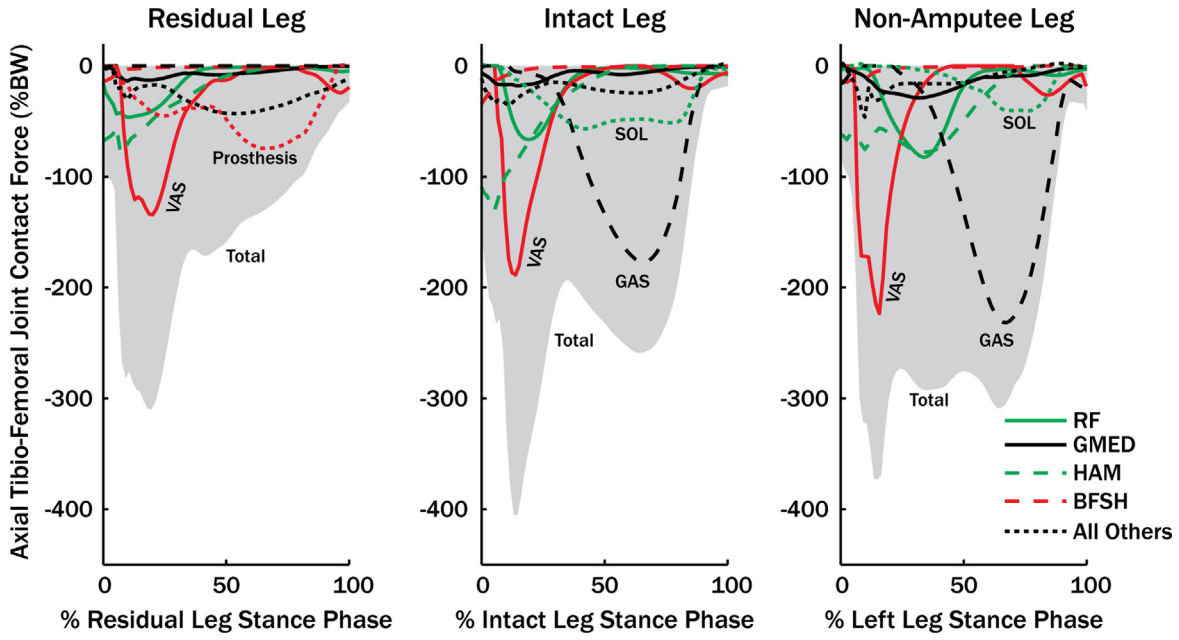

Fig. 2. Ipsilateral leg muscle group contributions to the axial tibio-femoral joint contact force over the stance phase. Forces are acting on the tibia and superior is defined as positive.

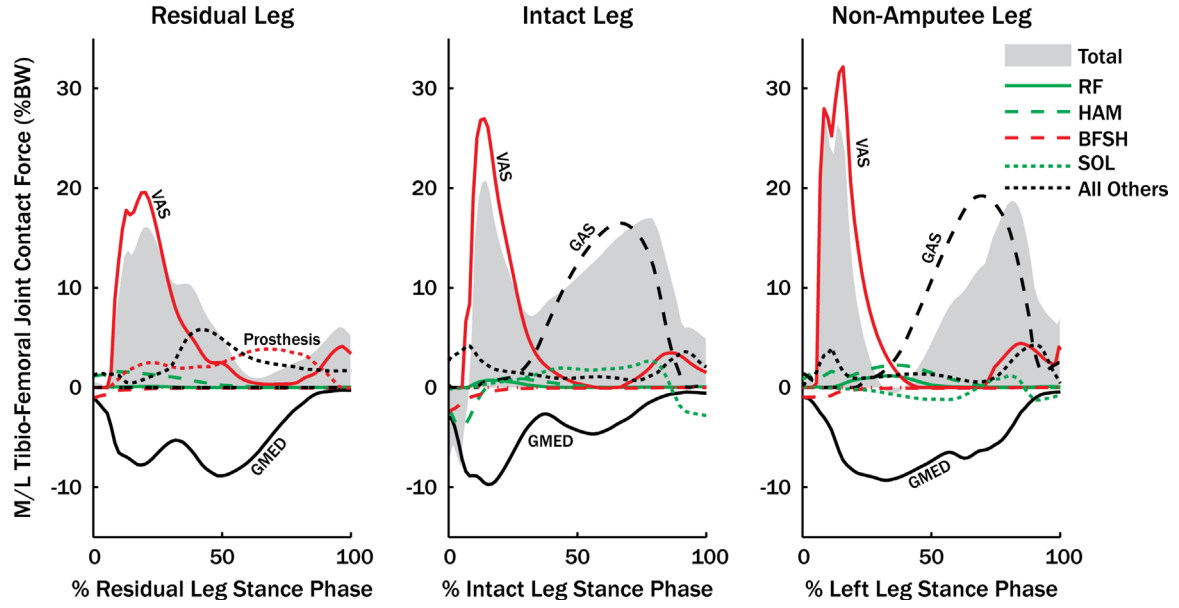

Fig. 3. Ipsilateral leg muscle group contributions to the mediolateral (*M*/*L*) tibio-femoral joint contact force over the stance phase. Forces are acting on the tibia and medial is defined as positive.

experimental results of greater hip extensor work in the intact leg in early stance (Silverman et al., 2008). Our results suggest that the peak contact force may be more important than the impulse in the development of OA and methods to reduce this peak force should be investigated. For example, training methods using biofeedback techniques to reduce the peak activity of intact leg HAM in early stance may be effective to reduce the peak knee contact force. However, increased activity of intact leg HAM may be needed to provide more body propulsion in early stance in amputees. Devices that reduce this compensation may potentially help reduce the prevalence of OA.

A potential limitation of this study is that the values of the peak knee joint contact force estimates in the simulations were higher compared to *in vivo* measurements using an instrumented tibio-femoral implant. *In vivo* peak knee axial force measurements are generally between 200% and 300% of body weight (D'Lima et al., 2008; Kutzner et al., 2013; Zhao et al., 2007a, 2007b). Experimental studies that have directly measured knee joint loads may be difficult to generalize to a larger group because of the small number of elderly subjects analyzed. While the peak knee joint contact forces in the simulations may be higher than expected, the load values for the majority of stance fall within expected ranges, and the relative loads between legs and individual muscle contributions to the knee joint loads still provide important insight into knee loading in amputee gait.

While joint loading is a major factor in OA development (Maly, 2009; Morgenroth et al., 2012), the etiology of OA is multifactorial. Bodyweight, prior trauma, joint laxity, joint malalignment and loading distribution are all risk factors for OA development (Suri et al., 2012). Thus, while the peak contact force in the axial direction

was highest in the intact leg, other biomechanical factors likely contribute to the development of OA in amputees. Interestingly, previous work has found that, at the hip, amputees have a much greater prevalence of OA in combination with reduced bone mineral density in the residual leg, although the prevalence of residual leg hip OA was much greater for transfemoral amputees compared to transtibial amputees (Kulkarni et al., 1998). These results highlight that joint loading alone likely does not fully explain increased prevalence of OA in this population, and other factors, such as vascular disruption, may accelerate disease progression.

An important area of future work is to examine the force distribution within the knee joint during amputee gait. Previous studies have compared the load distributions between the medial and lateral compartments in non-amputees and in general found that the medial compartment load is greater than the lateral compartment (Shelburne et al., 2006; Zhao et al., 2007a). Using a more complex model of the knee joint to analyze amputee walking may provide further insight in possible mechanisms that lead to the onset of OA in amputees. Another important area of future work is exploring variation in the knee contact force across individuals. The results from this study are representative of group average walking data using a generalized musculoskeletal model. Previous work has highlighted that individual participants use different movement strategies (e.g., Silverman et al., 2008) that may not be captured in average results. In addition, the musculoskeletal geometry of the residual limb and the function of the residual gastrocnemius may influence the residual leg joint loading. Thus, subject-specific models and simulations may provide further insight into how individual prosthetic devices, movement strategies and remaining residual leg musculature contribute to knee contact loading and eventual OA development.

5. Conclusion

The simulations showed the axial and M/L peak knee contact forces and stance phase knee impulses were smaller in the residual leg relative to the intact and non-amputee legs. In the axial direction, the peak knee contact force was higher in the intact leg relative to the non-amputee leg while the knee contact impulse was greater in the non-amputee leg. These results suggest that the peak knee contact force may be more important than the knee contact impulse in explaining the high prevalence of OA in the intact leg. Muscles that crossed the knee joint were the largest contributors to the joint forces including VAS, GAS and HAM. However, other muscles that do not cross the knee joint (e.g., SOL and GMED) and the prosthesis were large contributors to the knee contact forces through dynamic coupling. Future work investigating the contact force distribution in the knee joint during amputee gait may provide additional insight into the greater prevalence of OA in amputees.

Conflict of interest statement

There was no conflict of interest in the preparation or publication of this work.

Acknowledgments

This work was supported by the National Science Foundation Grant no. 0346514.

References

Anderson, F.C., 1999. A dynamic optimization solution for a complete cycle of normal gait. University of Texas at Austin.
Burke, M., Roman, V., Wright, V., 1978. Bone and joint changes in lower limb amputees. Ann. Rheum. Dis. 37, 252–254.
Culham, E.G., Peat, M., Newell, E., 1986. Below-knee amputation: a comparison of the effect of the SACH foot and single axis foot on electromyographic patterns during locomotion. Prosthet. Orthot. Int. 10, 15–22.
D'Lima, D.D., Steklov, N., Patil, S., Colwell, C.W., 2008. The Mark Coventry Award: In vivo knee forces during recreation and exercise after knee arthroplasty. Clin. Orthop. Relat. Res. 466, 2605–2611.
Davy, D.T., Audu, M.L., 1987. A dynamic optimization technique for predicting muscle forces in the swing phase of gait. J. Biomech. 20, 187–201.
Delp, S.L., Loan, J.P., Hoy, M.G., Zajac, F.E., Topp, E.L., Rosen, J.M., 1990. An interactive graphics-based model of the lower extremity to study orthopaedic surgical procedures. IEEE Trans. Biomed. Eng. 37, 757–767.
Fey, N.P., Neptune, R.R., 2012. Three-dimensional intersegmental knee joint forces and moments in below-knee amputees across steady-state walking speeds. Clin. Biomech. 27, 409–414.
Fey, N.P., Silverman, A.K., Neptune, R.R., 2010. The influence of increasing steady-state walking speed on muscle activity in below-knee amputees. J. Electromyogr. Kinesiol. 20, 155–161.
Goffe, W.L., Ferrier, G.D., Rogers, J., 1994. Global optimization of statistical functions with simulated annealing. J. Econ. 60, 65–99.
Isakov, E., Burger, H., Krajnik, J., Gregoric, M., Marincek, C., 2001. Knee muscle activity during ambulation of trans-tibial amputees. J. Rehabil. Med. 33, 196–199.
Isakov, E., Keren, O., Benjuya, N., 2000. Trans-tibial amputee gait: time-distance parameters and EMG activity. Prosthet. Orthot. Int. 24, 216–220.
Kulkarni, J., Adams, J., Thomas, E., Silman, A., 1998. Association between amputation, arthritis and osteopenia in British male war veterans with major lower limb amputations. Clin. Rehabil. 12, 348–353.
Kutzner, I., Stephan, D., Dymke, J., Bender, A., Graichen, F., Bergmann, G., 2013. The influence of footwear on knee joint loading during walking – in vivo load measurements with instrumented knee implants. J. Biomech. 46, 796–800.
Lemaire, E.D., Fisher, F.R., 1994. Osteoarthritis and elderly amputee gait. Arch. Phys. Med. Rehabil. 75, 1094–1099.
Lin, Y.C., Walter, J.P., Banks, S.A., Pandy, M.G., Fregly, B.J., 2010. Simultaneous prediction of muscle and contact forces in the knee during gait. J. Biomech. 43, 945–952.
Maly, M.R., 2009. Linking biomechanics to mobility and disability in people with knee osteoarthritis. Exerc. Sport Sci. Rev. 37, 36–42.
Melzer, I., Yekutiel, M., Sukenik, S., 2001. Comparative study of osteoarthritis of the contralateral knee joint of male amputees who do and do not play volleyball. J. Rheumatol. 28, 169–172.
Morgenroth, D.C., Gellhorn, A.C., Suri, P., 2012. Osteoarthritis in the disabled population: a mechanical perspective. PM R 4, S20–S7.
Neptune, R.R., Wright, I.C., Bogert, A.J., 2000. A method for numerical simulation of single limb ground contact events: application to heel-toe running. Comput. Methods Biomech. Biomed. Eng. 3, 321–334.
Nolan, L., Lees, A., 2000. The functional demands on the intact limb during walking for active trans-femoral and trans-tibial amputees. Prosthet. Orthot. Int. 24, 117–125.
Nolan, L., Wit, A., Dudzinski, K., Lees, A., Lake, M., Wychowanski, M., 2003. Adjustments in gait symmetry with walking speed in trans-femoral and trans-tibial amputees. Gait Posture 17, 142–151.
Norvell, D.C., Czerniecki, J.M., Reiber, G.E., Maynard, C., Pecoraro, J.A., Weiss, N.S., 2005. The prevalence of knee pain and symptomatic knee osteoarthritis among veteran traumatic amputees and nonamputees. Arch. Phys. Med. Rehabil. 86, 487–493.
Pinzur, M.S., Asselmeier, M., Smith, D., 1991. Dynamic electromyography in active and limited walking below-knee amputees. Orthopedics 14, 535–537.
Powers, C.M., Rao, S., Perry, J., 1998. Knee kinetics in trans-tibial amputee gait. Gait Posture 8, 1–7.
Raasch, C.C., Zajac, F.E., Ma, B., Levine, W.S., 1997. Muscle coordination of maximum-speed pedaling. J. Biomech. 30, 595–602.
Royer, T., Koenig, M., 2005. Joint loading and bone mineral density in persons with unilateral, trans-tibial amputation. Clin. Biomech. 20, 1119–1125.
Sanderson, D.J., Martin, P.E., 1997. Lower extremity kinematic and kinetic adaptations in unilateral below-knee amputees during walking. Gait Posture 6, 126–136.
Sasaki, K., Neptune, R.R., 2010. Individual muscle contributions to the axial knee joint contact force during normal walking. J. Biomech. 43, 2780–2784.
Shelburne, K.B., Torry, M.R., Pandy, M.G., 2006. Contributions of muscles, ligaments, and the ground-reaction force to tibiofemoral joint loading during normal gait. J. Orthop. Res. 24, 1983–1990.
Silverman, A.K., Fey, N.P., Portillo, A., Walden, J.G., Bosker, G., Neptune, R.R., 2008. Compensatory mechanisms in below-knee amputee gait in response to increasing steady-state walking speeds. Gait Posture 28, 602–609.
Silverman, A.K., Neptune, R.R., 2012. Muscle and prosthesis contributions to amputee walking mechanics: a modeling study. J. Biomech. 45, 2271–2278.
Struyf, P.A., van Heugten, C.M., Hitters, M.W., Smeets, R.J., 2009. The prevalence of osteoarthritis of the intact hip and knee among traumatic leg amputees. Arch. Phys. Med. Rehabil. 90, 440–446.

Suri, P., Morgenroth, D.C., Hunter, D.J., 2012. Epidemiology of osteoarthritis and associated comorbidities. PM R 4, pp. S10–S9.
Winby, C.R., Lloyd, D.G., Besier, T.F., Kirk, T.B., 2009. Muscle and external load contribution to knee joint contact loads during normal gait. J. Biomech. 42, 2294–2300.
Winter, D.A., Sienko, S.E., 1988. Biomechanics of below-knee amputee gait. J. Biomech. 21, 361–367.
Winters, J.M., Stark, L., 1988. Estimated mechanical properties of synergistic muscles involved in movements of a variety of human joints. J. Biomech. 21, 1027–1041.
Zajac, F.E., 1989. Muscle and tendon: properties, models, scaling, and application to biomechanics and motor control. Crit. Rev. Biomed. Eng. 17, 359–411.
Zajac, F.E., Neptune, R.R., Kautz, S.A., 2003. Biomechanics and muscle coordination of human walking: part II: lessons from dynamical simulations and clinical implications. Gait Posture 17, 1–17.
Zajac, F.E., Neptune, R.R., Kautz, S.A., 2002. Biomechanics and muscle coordination of human walking. Part I: introduction to concepts, power transfer, dynamics and simulations. Gait Posture 16, 215–232.
Zhao, D., Banks, S.A., D'Lima, D.D., Colwell, C.W., Fregly, B.J., 2007a. in vivo medial and lateral tibial loads during dynamic and high flexion activities. J. Orthop. Res. 25, 593–602.
Zhao, D., Banks, S.A., Mitchell, K.H., D'Lima, D.D., Colwell Jr., C.W., Fregly, B.J., 2007b. Correlation between the knee adduction torque and medial contact force for a variety of gait patterns. J. Orthop. Res. 25, 789–797.
Zmitrewicz, R.J., Neptune, R.R., Sasaki, K., 2007. Mechanical energetic contributions from individual muscles and elastic prosthetic feet during symmetric unilateral transtibial amputee walking: a theoretical study. J. Biomech. 40, 1824–1831.